

# A tunable high-Q millimeter wave cavity for hybrid circuit and cavity QED experiments

Cite as: Appl. Phys. Lett. **116**, 104001 (2020); <https://doi.org/10.1063/1.5137900>

Submitted: 18 November 2019 . Accepted: 05 March 2020 . Published Online: 13 March 2020

Aziza Suleymanzade , Alexander Anferov, Mark Stone, Ravi K. Naik , Andrew Oriani, Jonathan Simon, and David Schuster



View Online



Export Citation



CrossMark

## ARTICLES YOU MAY BE INTERESTED IN

### Development of microLED

Applied Physics Letters **116**, 100502 (2020); <https://doi.org/10.1063/1.5145201>

### Observing relaxation in device quality InGaN templates by TEM techniques

Applied Physics Letters **116**, 102104 (2020); <https://doi.org/10.1063/1.5139269>

### Periodical distribution of Au nanoparticles through dewetting on patterned substrates

Applied Physics Letters **116**, 103106 (2020); <https://doi.org/10.1063/1.5134145>

Lock-in Amplifiers  
Find out more today



Zurich  
Instruments



# A tunable high-Q millimeter wave cavity for hybrid circuit and cavity QED experiments

Cite as: Appl. Phys. Lett. **116**, 104001 (2020); doi: [10.1063/1.5137900](https://doi.org/10.1063/1.5137900)

Submitted: 18 November 2019 · Accepted: 5 March 2020 ·

Published Online: 13 March 2020





View Online



Export Citation



CrossMark

Aziza Suleymanzade,<sup>1,2</sup>  Alexander Anferov,<sup>1,2</sup> Mark Stone,<sup>1,2</sup> Ravi K. Naik,<sup>1,2</sup>  Andrew Oriani,<sup>1,3</sup> Jonathan Simon,<sup>1,2,3</sup> and David Schuster<sup>1,2,3,a)</sup>

## AFFILIATIONS

<sup>1</sup>Department of Physics, University of Chicago, Chicago, Illinois 60637, USA

<sup>2</sup>James Franck Institute, University of Chicago, Chicago, Illinois 60637, USA

<sup>3</sup>Pritzker School of Molecular Engineering, University of Chicago, Chicago, Illinois 60637, USA

<sup>a)</sup> Author to whom correspondence should be addressed: [azizas@uchicago.edu](mailto:azizas@uchicago.edu)

## ABSTRACT

The millimeter wave (mm-wave) frequency band provides exciting prospects for quantum science and devices since many high-fidelity quantum emitters, including Rydberg atoms, molecules, and silicon vacancies, exhibit resonances near 100 GHz. High-Q resonators at these frequencies would give access to strong interactions between emitters and single photons, leading to rich and unexplored quantum phenomena at temperatures above 1 K. We report a 3D mm-wave cavity with a measured single-photon internal quality factor of  $3 \times 10^7$  and mode volume of  $0.14 \times \lambda^3$  at 98.2 GHz, sufficient to reach strong coupling in a Rydberg cavity quantum electrodynamics system. An *in situ* piezo-tunability of 18 MHz facilitates coupling to specific atomic transitions. Our unique, seamless, and optically accessible resonator design is enabled by the realization that intersections of 3D waveguides support tightly confined bound states below the waveguide cutoff frequency. Harnessing the features of our cavity design, we realize a hybrid mm-wave and optical cavity, designed for interconversion and entanglement of mm-wave and optical photons using Rydberg atoms.

Published under license by AIP Publishing. <https://doi.org/10.1063/1.5137900>

Cavity and circuit Quantum Electrodynamics (QED) systems provide unprecedented control over photonic quantum states via coupling to strongly nonlinear single emitters. This effort began with pioneering works in Rydberg cavity QED, demonstrating first nonclassical micromaser radiation,<sup>1</sup> Schrödinger cat states, and early EPR experiments.<sup>2,3</sup> Since then, cavity and circuit QED systems have become essential tools for exploring quantum phenomena in both the optical<sup>4–7</sup> and microwave<sup>8,9</sup> regimes. Hybrid systems, which cross-couple these regimes, can harness the strengths of optical systems for communication and microwave systems for quantum information processing, yielding a more powerful toolset for quantum information technology.<sup>10</sup> In particular, the coherent interconversion of microwave and optical photons would enable large quantum networks and robust transfer of quantum information.<sup>11–18</sup>

Mm-wave frequencies provide a promising platform for hybrid quantum science<sup>19</sup> at less explored, but potentially beneficial length and energy scales. First, 100 GHz resonances with long coherence times are abundant among commonly used optical and microwave quantum emitters such as Rydberg atoms,<sup>20</sup> molecules,<sup>21</sup> and silicon vacancies<sup>22</sup> although they are rarely harnessed

for quantum science due to the lack of both high-Q resonators with tight mode confinement and mature mm-wave manipulation technology. Second, the mean thermal photon occupation of a 100 GHz resonator at 1 K is  $n_{ph} = 1 / (e^{h\nu/kT} - 1) = 0.009 \ll 1$ . This puts such a resonator in the quantum regime at temperatures accessible with simple pumped <sup>4</sup>He with much larger cooling powers and lower cost and complexity than the dilution refrigerators required to reach ~20 mK for 10 GHz experiments. Finally, the intermediate length scale of mm-waves enables the development of scalable high Q-factor devices using both near and far field wave engineering techniques.

More broadly, the mm-wave band is gaining interest across many fields of science and technology. Advances in mm-wave detection are essential for observational cosmology and the study of the cosmic microwave background.<sup>23,24</sup> Terahertz and near-terahertz radiation exhibits vast potential in hazardous chemical sensing and effective medical diagnostics.<sup>25,26</sup> Recently, the search for higher bandwidth and lower latency communication brought mm-wave wave frequencies into the focus of the telecommunication industry.<sup>27,28</sup> Once prohibitively limited and expensive, mm-wave technology is

becoming more available due to this progress, encouraging the development of mm-wave quantum devices.

Resonators with high  $Q$  values have been demonstrated, independently, in mm-wave,<sup>29</sup> optical,<sup>30,31</sup> and microwave<sup>32–34</sup> regimes with a few summarized in [supplementary material III](#). The pioneering work<sup>2,3</sup> with driven interactions between mm-wave photons and Rydberg atoms operated in large mode volume Fabry–Pérot-type resonators. While this enabled extremely high fidelity light-matter interactions, the interactions were slow and required optically inactive circular Rydberg atoms to achieve the necessary lifetimes. Working with optically accessible low angular momentum Rydbergs will require faster light-matter interactions achieved through a smaller mode volume, while still respecting the extreme sensitivity of Rydbergs to stray electric fields<sup>35</sup> by avoiding 2D resonator geometries.

In this work, we develop technology to hybridize mm-wave and optical photons for quantum science applications. We report a crossed optical and mm-wave cavity, with Rydberg atoms envisioned as a transducer. Our central breakthrough is the optically open, tunable 3D mm-wave cavity with  $Q = 3 \times 10^7$  and mode volume  $V = 0.14\lambda^3$  shown in [Fig. 1\(a\)](#).

In what follows, we first describe the design and manufacture of the seamless mm-wave cavity. We then introduce the mm-wave measurement setup in a 1 K cryostat and characterize the properties of the

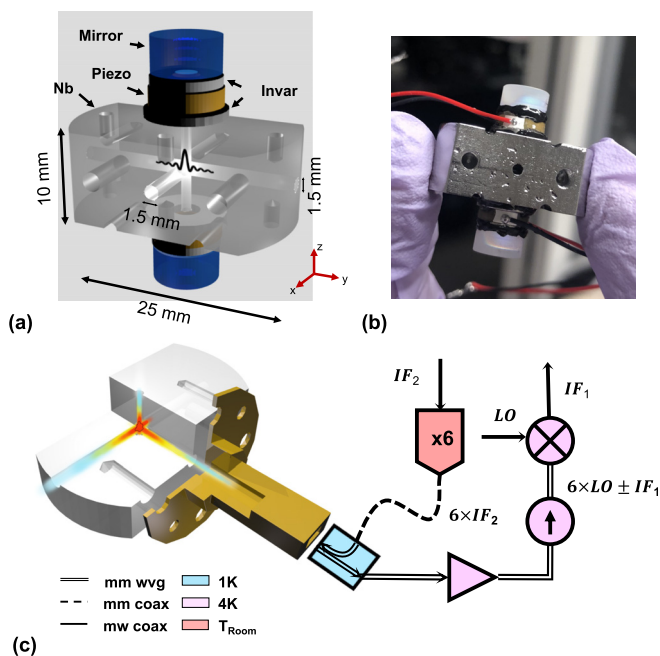


**FIG. 1.** (a) Schematic of crossed mm-wave and optical cavities. The superconducting mm-wave cavity is formed by the intersection of three evanescent waveguides. The x-axis waveguide will be employed for atom transport, y-axis waveguide for mm-wave coupling, and z-axis waveguide for an optical Fabry–Pérot cavity. Each side of the Fabry–Pérot cavity includes Invar spacers to prevent differential thermal contractions and a piezoactuator for tuning and locking the frequency of the optical cavity. (b) Photograph of the assembled crossed mm-wave and optical cavity with wired piezos. (c) Schematic reflection measurement setup for the mm-wave cavity. 100 GHz photons are delivered into the coupling port of the cavity through a WR10 waveguide.

device as a function of intra-cavity power and temperature. We also demonstrate *in situ* mechanical frequency control in the cryogenic environment. Finally, we discuss the application of this device in our Rydberg hybrid experiment and more broadly in cavity and circuit QED systems.

The key features of our device are its completely seamless design, sub-wavelength mode volume, and abundant optical access to the strongly confined mm-wave mode. Typically composed of two pieces, high- $Q$  3D cavities are vulnerable to photon leakage through the seam between the pieces,<sup>34</sup> which is more pronounced in cavities with shorter wavelengths. We create our mode by intersecting several evanescent tubes as shown in [Fig. 2](#). Since an intersection of any two dissimilar bodies creates a pocket with a larger cross section than each of them separately, this yields a bound state below the cutoff of the tubes. Indeed, any arbitrarily weak defect in 1D has this property,<sup>36</sup> albeit with weaker localization. The number of evanescent tubes and their diameters determines the frequency of the resonance, while the locations of each intersection and angles between the tubes control the localization of the lowest mode and symmetries of higher order modes. Coupling into the cavity is set by the diameter and length of the input and output tubes attached to the WR10 waveguides. These parameters fully specify the seamless cavity, leaving the internal quality factor as the sole unknown.

The flexibility of our design is demonstrated in [Fig. 2](#): using a single drill bit with a diameter below the cylindrical waveguide evanescent cutoff length  $\frac{1.841\lambda}{2\pi}$ , we are able to realize myriad resonator geometries with different spectra, depending on design requirements. The intersection of even two evanescent waveguides creates a well-localized mode at the “elbow” as shown in [Fig. 2\(a\)](#). Similarly, by intersecting more tubes in a “tee,” [Fig. 2\(b\)](#), or “star” configuration, [Fig. 2\(c\)](#), we trap light at lower frequencies for the same diameter of the tube. For diameter  $d = 1.6$  mm, a small number of tubes make conveniently sized high- $Q$  resonators at mm-wave frequencies. This approach could be applied to coupled cavities and lattices of resonators with open optical access for many-body physics with mm-wave photons and multiple emitters, both in 2D and 3D, as shown in [Fig. 2\(e\)](#). Finally,

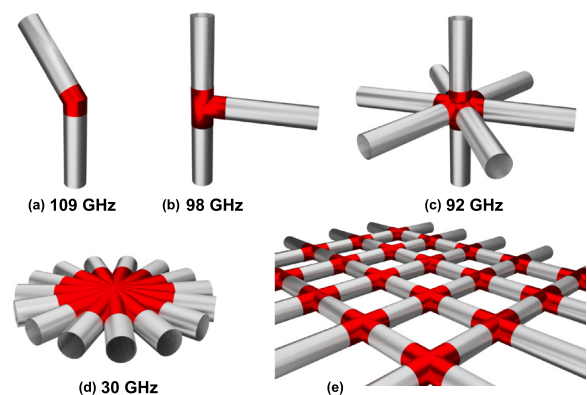


**FIG. 2.** Various seamless resonators made from intersecting 1.6 mm diameter tubes. The diameter of these tubes is chosen such that the low-frequency cutoff of each tube is  $\sim 110$  GHz. Examples of geometries with bound defect modes include the following: (a) an elbow resonator at 109 GHz made by intersection 2 tubes; (b) a 98 GHz tee; (c) 4-beam 92 GHz star; (d) a 30 GHz quasi-cylindrical resonator, made of 15 tubes; and (e) a 2D lattice of mm-wave “cross” resonators.

many intersecting tubes can create lower frequency microwave cavities as shown in Fig. 2(d), where one can approach a large, seamless cylindrical or rectangular volume by drilling out the cavity tube by tube. For the purposes of hybrid experiments, evanescent tubes have the advantage of providing optical access for optical Fabry–Pérot cavities, lasers, and atomic beams as shown in Fig. 1(a). All of these benefits make our design not only a powerful tool for hybrid Rydberg systems but also a flexible tool for other circuit and cavity QED systems.

The manufacturing of the device only involves drilling appropriate holes in high purity Niobium (Nb) stock. To reduce surface losses, the machined cavity is cleaned in solvents and chemically etched in a BCP bath of  $2\text{H}_3\text{PO}_4 : \text{HNO}_3 : \text{HF}$  for 20 min at room temperature.<sup>37</sup> After rinsing and drying, we immediately mount the cavity inside a Helium-4 adsorption cryostat to avoid surface degradation due to oxidation. The system is cooled down to 1 K, which is well below  $T_c = 9.2$  K of Nb, where the cavity is deep in the superconducting regime.

The 100 GHz measurement setup is shown in Fig. 1(c). It is analogous to traditional microwave measurement chains but with all components shifted to the 100 GHz band. This includes a Faraday isolator *Quinstar QIF-W*, cryogenic amplifier *LNF-LNC65-115WB*, and directional coupler *QJR-W-40-S*. For accessing the mm-wave band, we use a multiplier *VNAX-WR10* for upconversion and multiplier + mixer *VDI MixAMC 296* for downconversion. We characterize our cavities using  $S_{11}$  reflection measurement to fit both magnitude and phase and thereby extract quality factors and resonance frequencies. To test the capabilities of our design, we have made and characterized several mm-wave cavities shown in Fig. 3(a). By varying the length and diameter of the in-coupling port as well as number of tubes at the intersection point, we are able to create resonances of varying frequency and coupling Q [Fig. 3(b)]. We consistently measured internal quality factors in the tens of millions for BCP-etched cavities without etching the internal Qs are two orders of magnitude lower. All of these cavities have mode volumes below  $0.2\lambda^3$ , which allows a tight confinement of

mm-wave photons for tens of microseconds at 1 K using evanescence of the tubes alone.

For the hybrid mm-wave cavity crossed with an optical Fabry–Pérot cavity for our experiments with Rydberg atoms in Fig. 1(a), we created the mm-wave mode volume by intersecting three tubes, each with diameter 1.5 mm. We chose the precise dimensions of our resonator to match the  $35p$  to  $36s$  transition frequency of the  $^{85}\text{Rb}$  (see supplementary material II) and to avoid clipping of the laser and atomic beams transiting the mode in the experiment. We measured an internal quality factor of  $3 \times 10^7$  at 98.2 GHz, which corresponds to  $50 \mu\text{s}$  photon lifetime. To identify the loss channels limiting the lifetime of photons, we study how the internal quality factor depends on the power and temperature as shown in Figs. 3(c) and 3(d).

The internal quality factor of the resonator as a function of number of photons inside, shown in Fig. 3(c), reveals no power dependence from single photons to  $\sim 10\,000$  photons, indicating that our low-power Q is not limited by two-level system (TLS) absorbers, as is common in 2D resonators,<sup>38,39</sup> or that they remain unsaturated up to powers where other nonlinearities set in. We do observe a degradation in the quality factor and a nonlinear frequency response at high powers, suggesting the appearance of hot spots and metastable states on the surface of the etched Nb (see supplementary material I). As our primary interest lies in the performance of the cavity at single photon powers, we did not investigate this further.

Another common loss mechanism is surface resistivity due to thermal quasi-particles in the superconductor. Because this mechanism is known to be temperature dependent,<sup>40</sup> we are able to rule it out by examining the behavior of the resonator Q with temperature. In Fig. 3(d), we plot the temperature dependence of the fitted internal quality factor and fractional frequency change of the resonance for  $\sim 1$  and 9000 photons inside the cavity. The data are obtained by gradually heating and thermalizing the cavity using a power resistor. The internal quality factor as a function of temperature follows the

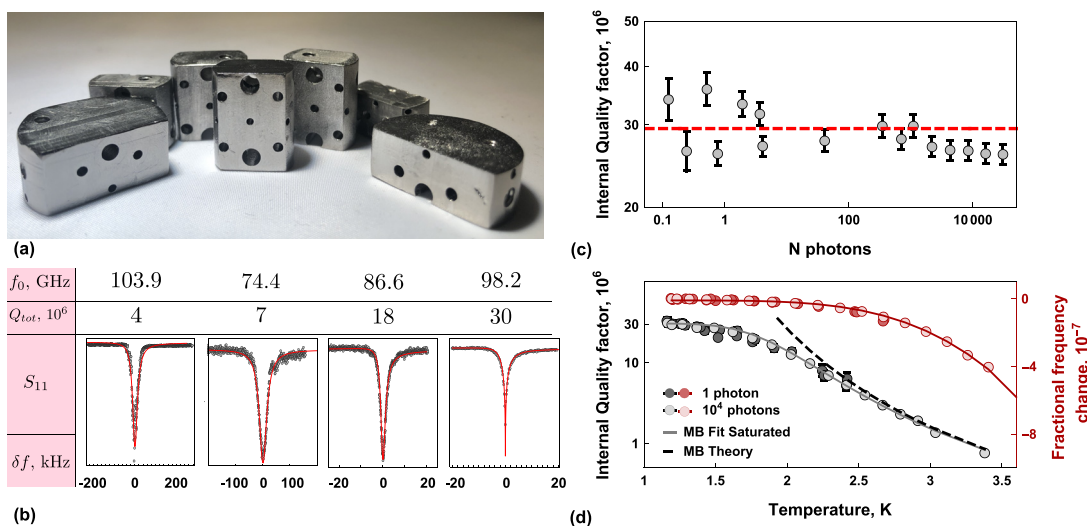


**FIG. 3.** (a) Photograph of various tested mm-wave cavity geometries. (b) Reflection spectra from several cavities with varying frequencies and coupling Q values, resulting in different total Q values. (c) Internal Q as a function of number of photons for the hybrid cavity. The constant trend indicates that the limiting loss mechanism is not power-dependent. (d) Internal Q (black) and fractional frequency change (red) as a function of temperature for the hybrid cavity. The deviation from Mattis–Bardeen curve at 2.3 K suggests that the resistivity of Nb does not limit the lifetime of the photons at the lowest temperatures.



Mattis–Bardeen law down to 2.3 K, where temperature-independent losses begin to dominate resulting in a deviation from the exponential trend. This indicates that we are not limited by thermal processes at the lowest temperatures.

In addition to these mechanisms, other potential loss channels include magnetic flux pinning<sup>41</sup> and photon leakage at the coupling boundary. The performance of the cavity could be further improved by adding magnetic field shielding<sup>42</sup> and sealing the rectangular to circular waveguide transition at the coupling port of the cavity to avoid leakage.

To precisely match the frequency of the cavity to an atomic transition, the cavity must be tunable. To achieve the desired accuracy, we follow several steps. First, we machine the cavity to within GHz accuracy. We design our resonator with a supplementary higher order mode with a low coupling Q that we can tune and measure at room temperature. Next, the cavity is etched in a BCP bath until we achieve sub-100 MHz accuracy. We are only able to reduce the frequency by etching, so we design the original device at a higher frequency than desired. The etching rate of MHz/min is quite reproducible as shown in [supplementary material IV](#). And, finally, we bring the resonator to the desired size before the cooldown using mechanical squeezing. During the cooldown, we can expect the frequency to shift on the order of 10 MHz due to thermal contraction, which is corrected using *in situ* tuning.

To achieve this, we thin one side of the cavity and pre-load a *Noliac* piezoelectric stack actuator as shown in [Figs. 4\(b\)](#) and [4\(c\)](#) to stress the cavity and thereby change its volume. Such stress-tuning provides several GHz of tunability at room-temperature, or  $\sim 18$  MHz at 1 K, as shown in [Fig. 4\(a\)](#). We note that while tunability is powerful, it has drawbacks: we observe that the thinning required to make the cavity tunable results in mechanical coupling to the pulse tube cryocooler vibrations, leading to fluctuations of the cavity frequency by

many linewidths. We also have access to tuning the Rydberg lines via AC polarizability using another cavity resonance in case the vibrations become limiting for the experiment.

For hybrid experiments with Rydberg atoms, the seamless mm-wave cavity enabled immediate integration with an optical Fabry–Pérot cavity with a waist  $w = 80 \mu\text{m}$  at 780 nm and measured optical finesse  $F = 10\,000$ . For quantum interconversion between optical and mm-wave bands, large collective cooperativities on both optical and mm-wave transitions are desirable;<sup>43</sup> large single-particle cooperativity on the mm-wave transition will be an enabling technology for quantum-nonlinear optics.<sup>44</sup> We compute single-particle cooperativities of  $C_{opt} = \frac{24F}{\pi} \frac{1}{(kw)^2} = 0.2$  and  $C_{mm} = 22\,000$  (see [supplementary material II](#)), which satisfy these constraints for a moderate-density atomic ensemble.<sup>45</sup>

In conclusion, we have designed and machined a tunable mm-wave cavity with a measured internal Q factor of  $3 \times 10^7$ . The seamless geometry tightly confines photons at the intersection of evanescent waveguides in the  $0.14\lambda^3$  mode volume, while allowing multiple lines-of-sight for optical access, injection of cold atoms, and integration with an optical cavity for quantum interconversion experiments.<sup>43,46</sup>

Our cavity Q values at 1 K are comparable to those of state-of-the-art 3D microwave ( $\sim 10$  GHz) cavities at 20 mK, which are conventionally integrated with transmon qubits.<sup>9,34</sup> We anticipate the possibility of interfacing our high-Q, high-frequency resonators with such 10 GHz transmons via 100 GHz nonlinear devices<sup>47,48</sup> employed as mixers.

For cavity and circuit QED, the tight confinement and long coherence of our device allows access to a strong coupling regime between a single photon and an emitter, which is difficult to achieve in many other platforms (see [supplementary material III](#)). The large cooperativity between a Rydberg atom and a mm-wave photon suggests studies of quantum many-body physics, photon-number-dependent group delay,<sup>44</sup> and vacuum-induced squeezing<sup>49</sup> on the mm-wave transition, while the effects can also be readout optically through the Fabry–Pérot cavity. In summary, this work heralds a promising era of optical/mm-wave quantum science.

See the [supplementary material](#) for (I) the observation and description of the nonlinear frequency response of the cavity at high powers, (II) the calculation of hybrid system cooperativities, (III) the comparisons with other state-of-the-art devices in the field, and (IV) the description of the frequency tuning of the cavity to match to the Rydberg states of atoms.

This work was primarily supported by the University of Chicago Materials Research Science and Engineering Center, which was funded by the National Science Foundation under Award No. DMR-1420709. This work was supported by ARO Grant No. W911NF-15-1-0397; D.S. acknowledges support from the David and Lucile Packard Foundation. A.S. acknowledges support in manuscript preparation from the Science Writing Practicum taught as part of U. Chicago’s “Data Science in Energy and Environmental Research” NRT training program, NSF Grant No. DGE-1735359.

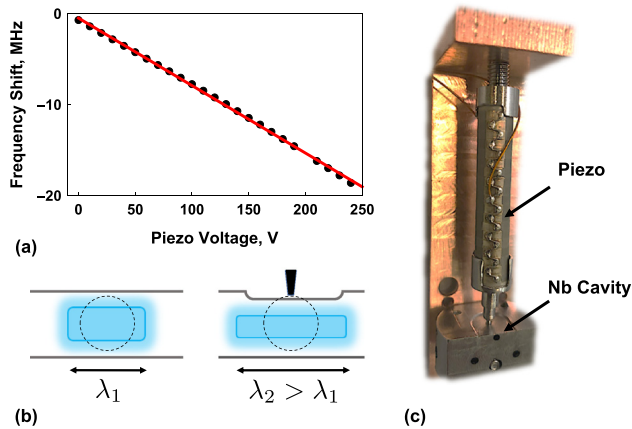


**FIG. 4.** Cryogenic frequency tuning of a high-Q mm-wave cavity. (a) Frequency shift of the cavity resonance as a function of piezovoltage. At 1 K, the linear fit shows  $\sim 0.1$  MHz/V tunability, with maximum frequency shift of  $\sim 18$  MHz. At room temperature, the increased piezostack enables cavity tuning by  $\sim$ GHz. (b) The low-temperature (1 K) tuning is accomplished by displacing a pre-thinned wall of the cavity by  $1\text{--}2 \mu\text{m}$  using a piezostack actuator. This pushes the mode farther out into the evanescent waveguides, effectively, increasing the wavelength and decreasing the frequency of the lowest mode. (c). Photograph of the piezoelectric actuator system attached to a test cavity.

## REFERENCES

- <sup>1</sup>G. Rempe, F. Schmidt-Kaler, and H. Walther, *Phys. Rev. Lett.* **64**, 2783 (1990).
- <sup>2</sup>M. Brune, F. Schmidt-Kaler, A. Maali, J. Dreyer, E. Hagley, J. M. Raimond, and S. Haroche, *Phys. Rev. Lett.* **76**, 1800 (1996).
- <sup>3</sup>J. M. Raimond, M. Brune, S. Haroche, and L. K. Brossel, *Rev. Mod. Phys.* **73**, 565 (2001).
- <sup>4</sup>K. M. Birnbaum, A. Boca, R. Miller, A. D. Boozer, T. E. Northup, and H. J. Kimble, *Nature* **436**, 87 (2005).
- <sup>5</sup>A. Boca, R. Miller, K. M. Birnbaum, A. D. Boozer, J. McKeever, and H. J. Kimble, *Phys. Rev. Lett.* **93**, 233603 (2004).
- <sup>6</sup>R. J. Thompson, G. Rempe, and H. J. Kimble, *Phys. Rev. Lett.* **68**, 1132 (1992).
- <sup>7</sup>A. Imamoglu, D. D. Awschalom, G. Burkard, D. P. DiVincenzo, D. Loss, M. Sherwin, and A. Small, *Phys. Rev. Lett.* **83**, 4204 (1999).
- <sup>8</sup>A. Wallraff, D. I. Schuster, A. Blais, L. Frunzio, R.-S. Huang, J. Majer, S. Kumar, S. M. Girvin, and R. J. Schoelkopf, *Nature* **431**, 162 (2004).
- <sup>9</sup>H. Paik, D. I. Schuster, L. S. Bishop, G. Kirchmair, G. Catelani, A. P. Sears, B. R. Johnson, M. J. Reagor, L. Frunzio, L. I. Glazman *et al.*, *Phys. Rev. Lett.* **107**, 240501 (2011).
- <sup>10</sup>T. D. Ladd, F. Jelezko, R. Laflamme, Y. Nakamura, C. Monroe, and J. L. O'Brien, *Nature* **464**, 45 (2010).
- <sup>11</sup>R. W. Andrews, R. W. Peterson, T. P. Purdy, K. Cicak, R. W. Simmonds, C. A. Regal, and K. W. Lehnert, *Nat. Phys.* **10**, 321 (2014).
- <sup>12</sup>J. T. Hill, A. H. Safavi-Naeini, J. Chan, and O. Painter, *Nat. Commun.* **3**, 1196 (2012).
- <sup>13</sup>J. Bochmann, A. Vainsencher, D. D. Awschalom, and A. N. Cleland, *Nat. Phys.* **9**, 712 (2013).
- <sup>14</sup>M. Forsch, R. Stockill, A. Wallucks, I. Marinkovic, C. Gärtner, R. A. Norte, F. van Otten, A. Fiore, K. Srinivasan, and S. Gröblacher, *arXiv:1812.07588* (2018).
- <sup>15</sup>A. Vainsencher, K. J. Satzinger, G. A. Peairs, and A. N. Cleland, *Appl. Phys. Lett.* **109**, 033107 (2016).
- <sup>16</sup>B. Abdo, K. Sliwa, F. Schackert, N. Bergeal, M. Hatridge, L. Frunzio, A. D. Stone, and M. Devoret, *Phys. Rev. Lett.* **110**, 173902 (2013).
- <sup>17</sup>M. Hafezi, Z. Kim, S. L. Rolston, L. A. Orozco, B. L. Lev, and J. M. Taylor, *Phys. Rev. A* **85**, 020302 (2012).
- <sup>18</sup>M. Kiffner, A. Feizpour, K. T. Kaczmarek, D. Jaksch, and J. Nunn, *New J. Phys.* **18**, 093030 (2016).
- <sup>19</sup>M. Pechal and A. H. Safavi-Naeini, *Phys. Rev. A* **96**, 042305 (2017).
- <sup>20</sup>W. Li, I. Mourachko, M. W. Noel, and T. F. Gallagher, *Phys. Rev. A* **67**, 052502 (2003).
- <sup>21</sup>Y. Zhou, D. D. Grimes, T. J. Barnum, D. Patterson, S. L. Coy, E. Klein, J. S. Muentner, and R. W. Field, *Chem. Phys. Lett.* **640**, 124 (2015).
- <sup>22</sup>D. Sukachev, A. Sipahigil, C. Nguyen, M. Bhaskar, R. Evans, F. Jelezko, and M. Lukin, *Phys. Rev. Lett.* **119**, 223602 (2017).
- <sup>23</sup>J. E. Carlstrom, P. A. R. Ade, K. A. Aird, B. A. Benson, L. E. Bleem, S. Buseti, C. L. Chang, E. Chauvin, H.-M. Cho, T. M. Crawford *et al.*, *Publ. Astron. Soc. Pacific* **123**, 568 (2011).
- <sup>24</sup>J. D. Vieira, T. M. Crawford, E. R. Switzer, P. A. R. Ade, K. A. Aird, M. L. N. Ashby, B. A. Benson, L. E. Bleem, M. Brodwin, J. E. Carlstrom *et al.*, *Astrophys. J.* **719**, 763 (2010).
- <sup>25</sup>P. Jepsen, D. Cooke, and M. Koch, *Laser Photonics Rev.* **5**, 124 (2011).
- <sup>26</sup>F. Sizov, *Semicond. Sci. Technol.* **33**, 123001 (2018).
- <sup>27</sup>T. S. Rappaport, S. Sun, R. Mayzus, H. Zhao, Y. Azar, K. Wang, G. N. Wong, J. K. Schulz, M. Samimi, and F. Gutierrez, *IEEE Access* **1**, 335 (2013).
- <sup>28</sup>W. Roh, J. Seol, J. Park, B. Lee, J. Lee, Y. Kim, J. Cho, K. Cheun, and F. Aryanfar, *IEEE Commun. Mag.* **52**, 106 (2014).
- <sup>29</sup>S. Kuhr, S. Gleyzes, C. Guerlin, J. Bernu, U. B. Hoff, S. Deléglise, S. Osnaghi, M. Brune, J.-M. Raimond, S. Haroche *et al.*, *Appl. Phys. Lett.* **90**, 164101 (2007).
- <sup>30</sup>D. Hunger, T. Steinmetz, Y. Colombe, C. Deutsch, T. W. Hänsch, and J. Reichel, *New J. Phys.* **12**, 065038 (2010).
- <sup>31</sup>K. J. Vahala, *Nature* **424**, 839 (2003).
- <sup>32</sup>A. Romanenko and D. Schuster, *Phys. Rev. Lett.* **119**, 264801 (2017).
- <sup>33</sup>H. G. Leduc, B. Bumble, P. K. Day, B. H. Eom, J. Gao, S. Golwala, B. A. Mazin, S. McHugh, A. Merrill, D. C. Moore *et al.*, *Appl. Phys. Lett.* **97**, 102509 (2010).
- <sup>34</sup>M. Reagor, H. Paik, G. Catelani, L. Sun, C. Axline, E. Holland, I. M. Pop, N. A. Masluk, T. Brecht, L. Frunzio *et al.*, *Appl. Phys. Lett.* **102**, 192604 (2013).
- <sup>35</sup>H. Hattermann, M. Mack, F. Karlewski, F. Jessen, D. Cano, and J. Fortágh, *Phys. Rev. A* **86**, 022511 (2012).
- <sup>36</sup>K. Chadani, N. Khuri, A. Martin, and T. Tsun Wu, *J. Math. Phys.* **44**, 406 (2003).
- <sup>37</sup>H. Tian, C. E. Reece, M. J. Kelley, S. Wang, L. Plucinski, K. E. Smith, and M. Nowell, *Appl. Surf. Sci.* **253**, 1236 (2006).
- <sup>38</sup>M. S. Khalil, F. C. Wellstood, and K. D. Osborn, *IEEE Trans. Appl. Supercond.* **21**, 879 (2011).
- <sup>39</sup>J. M. Martinis, K. B. Cooper, R. McDermott, M. Steffen, M. Ansmann, K. D. Osborn, K. Cicak, S. Oh, D. P. Pappas, R. W. Simmonds *et al.*, *Phys. Rev. Lett.* **95**, 210503 (2005).
- <sup>40</sup>A. Gurevich, *Superconductor Sci. Technol.* **30**, 034004 (2017).
- <sup>41</sup>A. Romanenko, A. Grassellino, A. C. Crawford, D. A. Sergatskov, and O. Melnychuk, *Appl. Phys. Lett.* **105**, 234103 (2014).
- <sup>42</sup>M. Ono, E. Kako, K. Saito, T. Shishido, S. Noguchi, and T. Yokoi, in 9th Workshop on RF Superconductivity (1999).
- <sup>43</sup>J. P. Covey, A. Sipahigil, and M. Saffman, *Phys. Rev. A* **100**, 012307 (2019).
- <sup>44</sup>G. Nikoghosyan and M. Fleischhauer, *Phys. Rev. Lett.* **105**, 013601 (2010).
- <sup>45</sup>J. Ningyuan, A. Georgakopoulos, A. Ryou, N. Schine, A. Sommer, and J. Simon, *Phys. Rev. A* **93**, 041802 (2016).
- <sup>46</sup>B. T. Gard, K. Jacobs, R. McDermott, and M. Saffman, *Phys. Rev. A* **96**, 013833 (2017).
- <sup>47</sup>A. Anferov, A. Suleymanzade, A. Oriani, J. Simon, and D. I. Schuster, *arXiv:1909.01487* (2019).
- <sup>48</sup>S. V. Lotkhov, R. Dolata, and M. Khabipov, *arXiv:1909.02349* (2019).
- <sup>49</sup>J. Hu, W. Chen, Z. Vendeiro, A. Urvoy, B. Braverman, and V. Vuletić, *Phys. Rev. A* **96**, 050301 (2017).